JOURNAL OF EXPERIMENTAL ZOOLOGY (MOL DEV EVOL) 312B:292–308 (2009)

# Revitalization of a Diastemal Tooth Primordium in *Spry2* Null Mice Results From Increased Proliferation and Decreased Apoptosis

RENATA PETERKOVA[1]*, SVATAVA CHURAVA[1,2], HERVE LESOT[3–5], MICHAELA ROTHOVA[1,6], JAN PROCHAZKA[1,6], MIROSLAV PETERKA[1,2], AND OPHIR D. KLEIN[7–9]*

[1]*Department of Teratology, Institute of Experimental Medicine, Academy of Sciences of the Czech Republic, Prague, Czech Republic*

[2]*Department of Anthropology, Faculty of Science, Charles University, Prague, Czech Republic*

[3]*INSERM U595, Faculté de Médecine, Université Louis Pasteur, Strasbourg, France*

[4]*Faculté de Chirurgie Dentaire, Université Louis Pasteur, Strasbourg, France*

[5]*International Collaborating Centre in Oro-Facial Genetics and Development, University of Liverpool, Liverpool, United Kingdom*

[6]*Department of Developmental Biology, Faculty of Science, Charles University, Prague, Czech Republic*

[7]*Department of Orofacial Sciences, University of California, San Francisco, California*

[8]*Department of Pediatrics, University of California, San Francisco, California*

[9]*Institutes of Human Genetics and Regeneration Medicine, University of California, San Francisco, California*

*ABSTRACT* An understanding of the factors that promote or inhibit tooth development is essential for designing biological tooth replacements. The embryonic mouse dentition provides an ideal system for studying such factors because it consists of two types of tooth primordia. One type of primordium will go on to form a functional tooth, whereas the other initiates development but arrests at or before the bud stage. This developmental arrest contributes to the formation of the toothless mouse diastema. It is accompanied by the apoptosis of the rudimentary diastemal buds, which presumably results from the insufficient activity of anti-apoptotic signals such as fibroblast growth factors (FGFs). We have previously shown that the arrest of a rudimentary tooth bud can be rescued by inactivating *Spry2*, an antagonist of FGF signaling. Here, we studied the role of the epithelial cell death and proliferation in this process by comparing the development of a rudimentary diastemal tooth bud ($R_2$) and the first molar in the mandibles of *Spry2*$^{-/-}$ and wild-type (WT) embryos using histological sections, image analysis and 3D reconstructions. In the WT $R_2$ at embryonic day 13.5, significantly increased apoptosis and decreased proliferation were found compared with the first molar. In contrast, increased levels of FGF signaling in *Spry2*$^{-/-}$ embryos led to significantly decreased apoptosis and increased proliferation in the $R_2$ bud. Consequently, the $R_2$ was involved in the formation of a supernumerary tooth primordium. Studies of the revitalization of

Grant sponsor: Grant Agency of the Czech Republic; Grant numbers: 304/05/2665; and 304/07/0223; Grant sponsor: Ministry of Education, Youth and Sports of the Czech Republic; Grant numbers: MSM0021620843; and COST B23.002; Grant sponsor: U.C.S.F. Sandler Family Foundation; Grant sponsor: NIH; Grant number: K08-DE017654.

*Correspondence to: Renata Peterkova, Department of Teratology, Institute of Experimental Medicine, Academy of Sciences of the Czech Republic, v.v.i., Videnska 1083, 14220 Prague, Czech Republic. E-mail: repete@biomed.cas.cz; Ophir D. Klein, Departments of Orofacial Sciences and Pediatrics, University of California, San Francisco, CA 94143-0442 USA. E-mail: Ophir.Klein@ucsf.edu

Received 19 November 2008; Accepted 20 November 2008
Published online 6 January 2009 in Wiley InterScience (www.interscience.wiley.com). DOI: 10.1002/jez.b.21266

rudimentary tooth primordia in mutant mice can help to lay the foundation for tooth regeneration by enhancing our knowledge of mechanisms that regulate tooth formation. *J. Exp. Zool. (Mol. Dev. Evol.) 312B:292–308, 2009.* 

**How to cite this article: Peterkova R, Churava S, Lesot H, Rothova M, Prochazka J, Peterka M, Klein OD. 2009. Revitalization of a diastemal tooth primordium in *Spry2* null mice results from increased proliferation and decreased apoptosis. J. Exp. Zool. (Mol. Dev. Evol.) 312B:292–308.**

The mouse embryonic dentition provides a natural model for studying the factors that support or inhibit tooth development, as it contains not only germs of functional teeth but also several types of rudimentary tooth primordia (Fig. 1). These rudiments undergo the initial stages of tooth morphogenesis but then are repressed, either through regression or by merging with primordia of functional dentition. These rudimentary primordia have been hypothesized to represent vestiges of ancestral teeth that were suppressed during evolution (Peterkova et al., 2000, 2002a). The coexistence of rudimentary primordia and primordia of prospective functional teeth in the jaw allows comparison of the molecular control of their development in the same animal as well as between wild-type (WT) and mutant mice. The observation that these rudiments can form functional teeth in mutant mice also raises the stimulating possibility that these structures can serve as models of controlled tooth regeneration (Peterkova et al., 2006; D'Souza and Klein, 2007).

Adult mice have a greatly reduced number of teeth compared with other mammals. In each jaw quadrant, they have only one incisor and three molars (Fig. 1A). The incisor and molars are separated by a toothless gap (diastema) where other mammals have incisors, canines and premolars. The embryonic mouse diastema transiently contains the above-mentioned rudimentary (vestigial) tooth primordia (Fig. 1B). The most prominent of these rudiments are two large buds that are present in the posterior part of the diastema, just anterior to the first molar, in each maxilla or mandible. These two rudiments are initially even larger than the first molar itself, and therefore can be mistaken for the first molar primordium at early stages. However, the development of these large diastemal buds ceases before the cap stage, and programmed cell death (apoptosis) occurs in their epithelium (Peterkova et al., '96, 2000; Viriot et al., 2000). These large rudimentary buds have been homologized to the premolars lost during mouse evolution (Peterkova et al., 2000; Viriot et al., 2002).

Mutations in both ectodysplasin (*Eda*) and sprouty (*Spry*) genes can stimulate the revival of the large diastemal buds leading to the development of a supernumerary cheek tooth in front of the first molar (Peterkova et al., 2005; Klein et al., 2006). Such a supernumerary tooth can be thought of as a tooth atavism because it is located in the position of a lost premolar (Peterkova et al., 2005, 2006).

Sprouty genes encode negative feedback antagonists of signaling by fibroblast growth factors (FGFs) and other receptor-tyrosine kinase ligands (Minowada et al., '99). The FGF signaling pathway is evolutionarily conserved and plays crucial roles in the development of many craniofacial structures, including teeth (Nie et al., 2006). The effect of decreased FGF signaling during tooth development has been studied in mouse embryos lacking the epithelium-specific b-isoform of FGF receptor 2. In such mice, tooth development is arrested at the bud stage (Celli et al., '98). In contrast to FGF receptor mutants, in sprouty null mice FGF signaling is increased which leads to several abnormalities in tooth development (Klein et al., 2006, 2008). In WT mice, *Spry2* and *Spry4* are expressed in different tissue compartments during early tooth development: *Spry2* in the epithelium and *Spry4* in the mesenchyme. In mice carrying mutations in either *Spry2* or *Spry4*, supernumerary teeth develop in front of the first lower molars as a result of the abnormal survival and development of diastemal tooth buds (Klein et al., 2006).

Apoptosis is involved in the repression of the development of the large rudimentary tooth buds in the posterior part of the diastema in WT mice at embryonic day (ED) 12.5–13.5 (Peterkova et al., '96; Viriot et al., 2000) (Fig. 1B). We have proposed that apoptosis in dental epithelium is stimulated by a relative predominance of growth inhibitors (Fig. 1C), and that a relative increase in growth activators (e.g. FGFs) can downregulate apoptosis and support further growth (Peterkova et al., 2003). Therefore, we set out to test the following hypothesis: the absence of an FGF antagonist leads to the abnormal survival of diastemal tooth

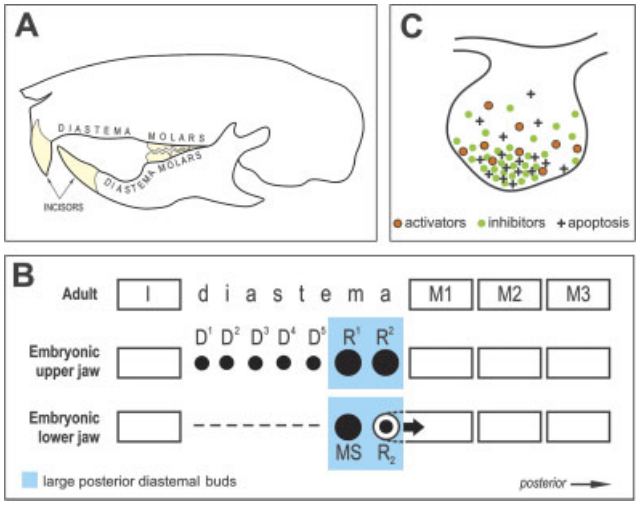


Fig. 1. Schematic of tooth pattern in the adult and embryonic mouse and a model of apoptosis regulation in tooth buds. (**A**) Each quadrant of the adult mouse dentition has one incisor and three molars separated by a toothless diastema. (**B**) Schematic of tooth pattern in one jaw quadrant in adult and embryonic mouse. In the anterior part of the embryonic diastema, either rudimentary small placodes/buds ($D^1$–$D^5$) or an epithelial thickening (dashed line) develops in the maxilla or mandible, respectively, until ED 13.0, at which point they start to disappear (Peterkova et al., '95; Lesot et al., '99). In the posterior part of the diastema, two large rudimentary buds consecutively appear and become the most prominent tooth primordia in the cheek region at ED 12.5 and 13.5, respectively ($R^1$ and $R^2$ in the maxilla; MS and $R_2$ in the mandible), before their development ceases. After ED 13.0, $R^1$, $R^2$ and MS regress, whereas the $R_2$ bud is incorporated (large arrow) into the anterior part of the first molar cap (Peterkova et al., '96; Viriot et al., 2000). The remnants of $R^1$, $R^2$ and MS are thought to contribute during later morphogenesis to expansion of the first molar (Lesot et al., '96; Peterkova et al., 2005). Black spots indicate the primordia affected by programmed cell death (apoptosis), which occurs during elimination of $D^1$–$D^5$, regression of $R^1$, $R^2$ and MS and growth retardation of $R_2$ (Tureckova et al., '96; Peterkova et al., '96; Viriot et al., 2000). The upper mouse incisor originates from five to six tooth placodes, whereas three placodes might occur in the lower incisor region at initial stages (Peterkova et al., 2002a) (not shown). I, incisor; M1, M2, M3, first, second and third molars, respectively. (**C**) A model for the regulation of apoptosis at the tip of a tooth bud by interaction between growth activators (e.g. FGFs) and inhibitors (e.g. BMPs). A local excess of inhibitors leads to the epithelial cells' failure to receive adequate growth-activating (apoptosis-suppressing) signals (e.g. FGF). This signaling imbalance (relative predominance of inhibitors) can stimulate apoptosis (modified from Peterkova et al., 2003). ED, embryonic day; FGF, fibroblast growth factor; BMP, bone morphogenetic protein.

buds in *Spry2* null embryos by causing decreased apoptosis and increased proliferation, thus preventing the growth arrest that normally occurs in these rudiments. We compared the development of the posterior diastemal bud ($R_2$) and the molar epithelium in the mandible of *Spry2*$^{-/-}$ and WT mice using histological sections, 3D reconstructions, morphometry and quantitative evaluation of proliferation and apoptosis.

## MATERIALS AND METHODS

### *Mouse lines and staging of embryos*

Mouse lines carrying mutant alleles of *Spry2* were maintained and genotyped as reported (Shim et al., 2005). The females were mated overnight and noon after the detection of the vaginal plug was considered as ED 0.5. The pregnant mice were killed by cervical dislocation and their offspring were harvested at ED 13.5, 14.0, 14.5 and 15.5. Immediately after taking the embryo out of the uterus, the drop of amniotic fluid on its surface was gently removed by dabbing on a filter paper and the wet body weight was determined (Peterka et al., 2002). Each embryo was individually put in a bottle with Bouin fluid and fixed at room temperature for 10 days. Age/body weight-matched WT embryos were used as controls.

### *Histology*

We processed 14 WT and 14 mutant embryonic heads at ED 13.5–15.5 for histology. Heads were embedded in paraffin, cut in 7 μm frontal serial sections and stained with a modified Mallory method (alcian blue–hematoxylin–eosin) (Fig. 2).

### *3D reconstructions of dental epithelium and apoptosis distribution*

Computer-aided 3D reconstructions of the developing lower cheek dentition were made in age/weight-matched pairs of *Spry2*$^{-/-}$ and WT mice at ED 13.5, 14.0, 14.5 and 15.5 (Fig. 3). Contours of the dental and adjacent oral epithelium were drawn from histological sections at 7 μm intervals using a Leica DMLB microscope (Leica Microsystems GmbH, Wetzlar, Germany) equipped with a drawing chamber at a magnification of 320 ×. At ED 13.5, apoptotic cells and bodies (Fig. 2A) were identified in the dental epithelium on histological sections based on morphological criteria (Tureckova et al., '96). These were recorded into a drawing and distinguished according to their position in one of the following three regions of dental epithelium: the superficial zone (thickness similar to the adjacent oral epithelium), the internal

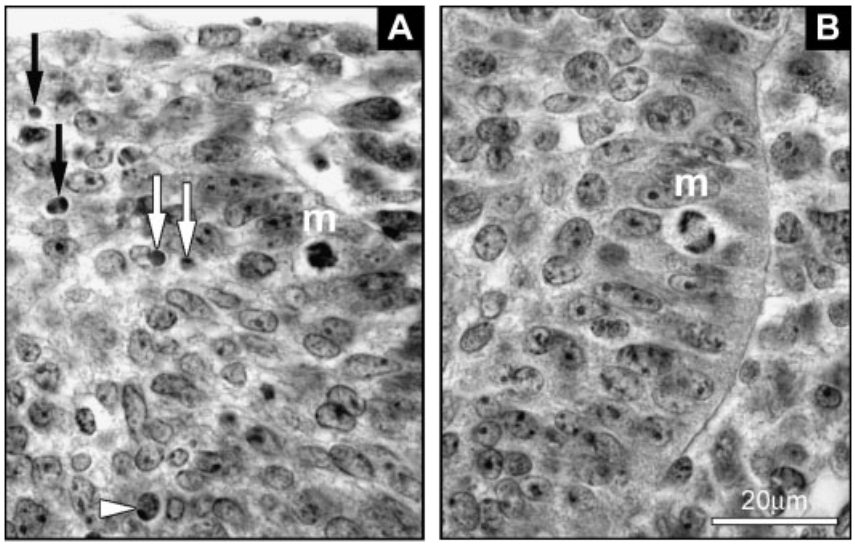


Fig. 2. Histological pictures of apoptosis and mitosis in the dental epithelium. (**A**) Examples of an apoptotic cell (arrowhead) and apoptotic bodies (white and black arrows) in the $R_2$ rudiment. m, mitosis. (**B**) A mitotic cell (m) in molar epithelium.

zone and the enamel knot zone (Fig. 4), corresponding to blue, white and red spots, respectively (see Fig. 6). The digitalization of the serial drawings, the correlation of successive images and the generation of 3D pictures have been previously described (Lesot et al., '96).

### *Morphometry of dental epithelium*

The size of the dental epithelium was compared in age/weight-matched pairs of *Spry2*$^{-/-}$ and WT embryos at ED 13.5, 14.0 and 14.5 (Fig. 5). We employed the same specimens that were used for 3D reconstructions. The area of the dental epithelium on frontal sections in the cheek region of the mandible was measured on every fifth section (i.e. at 35 μm intervals) along the antero-posterior jaw axes (Fig. 5). The first evaluated section was the one in which the lingual side of the infolding of the dental epithelium and the adjacent oral epithelium were at an angle close to or less than 90°. The last evaluated section was the one in which the dental epithelium still protruded into the mesenchyme.

We measured the frontal section area of the dental epithelium (at a magnification of 1,250 ×) on digitalized images made by Leica DMLB microscope (Leica Microsystems GmbH, Wetzlar, Germany) equipped with a camera Leica DC480 (Leica Microsystems GmbH, Wetzlar, Germany) using PC software ImageJ (http://rsb.info.nih.gov/ij/). The measured area was delimited by the basement membrane, the oral surface of the epithelium and by the places where the thickness of the dental epithelium decreased to the thickness of the medially and laterally adjacent oral epithelium. The values were converted to $\mu m^2$ and plotted (Fig. 5).

### *Quantitative evaluation of apoptosis*

We analyzed the number of apoptotic cells and bodies (Fig. 2A) in the posterior diastemal bud $R_2$ and the molar epithelium in *Spry2*$^{-/-}$ and WT embryos at ED 13.5 (Fig. 7, Table 1). In order to compare WT and mutant tooth primordia at similar stage of odontogenesis, we selected from among ED 13.5 embryos one group of WT and one group of *Spry2*$^{-/-}$ embryos of similar body weight. The embryonic body weight has been shown to correlate very well with the stage of mouse tooth development (Peterka et al., 2002). The control group was composed of ten right and left lower jaw quadrants of five WT embryos (weight range 154–178 mg), and the mutant group was composed of six right and left jaw quadrants of three mutant embryos (weight range 167–182 mg) (Table 1).

In each lower jaw quadrant, apoptosis was analyzed in two segments of the dental epithelium representing the $R_2$ diastemal bud and the molar epithelium (Fig. 7). Each segment comprised ten consecutive 7 μm thick histological sections. The segments were separated by a gap of 70 μm (ten sections). The boundaries of the segments were determined on the basis of the position of the middle of the $R_2$ segment. This corresponded to a section with the most pronounced enamel knot at the tip of the bud $R_2$ (compare with Fig. 4).

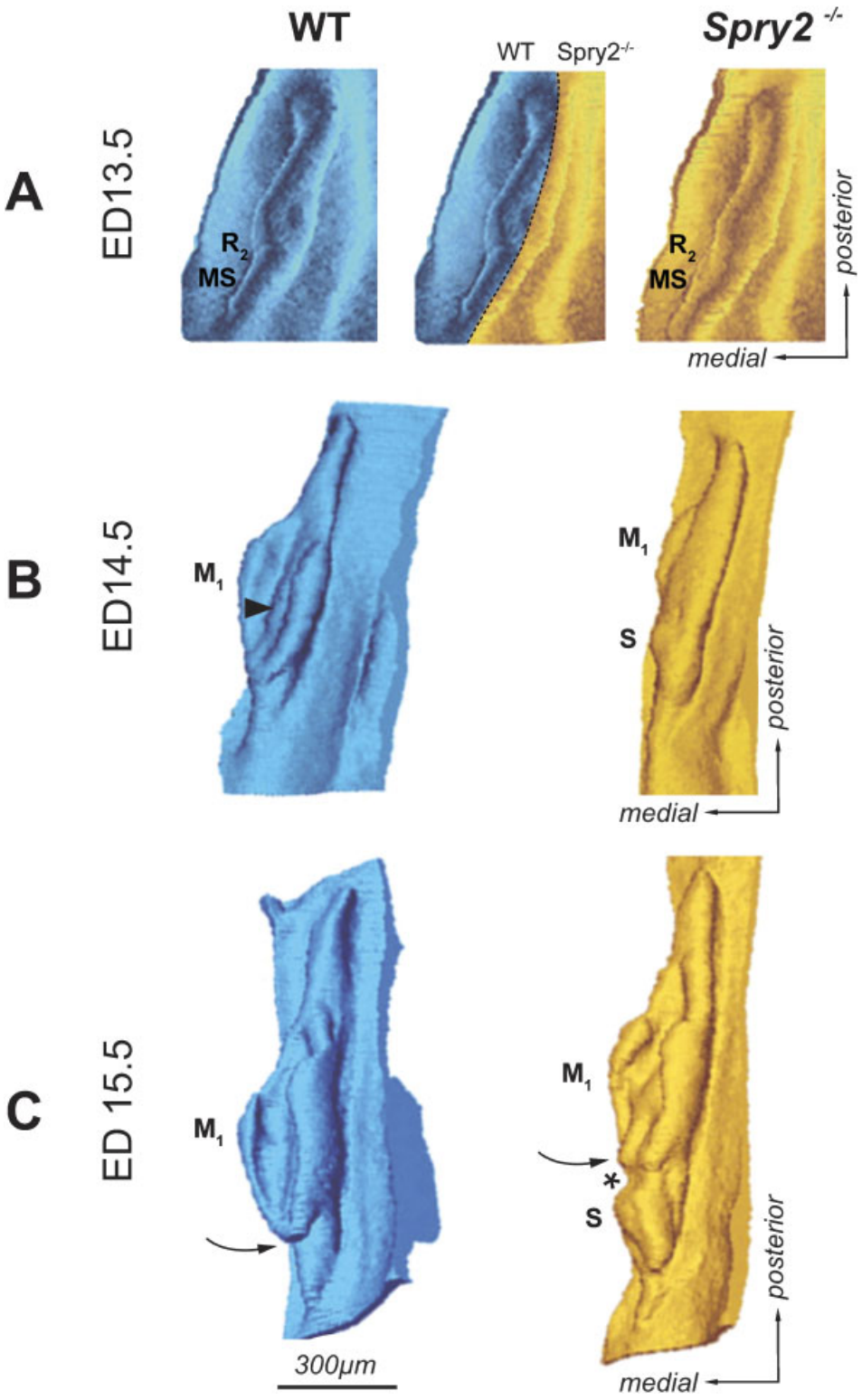


Fig. 3. Three-dimensional reconstructions of the dental epithelium. Mesenchymal view of the dental and adjacent oral epithelium in the cheek region of the mandible is presented in (**A**) aerial and (**B**, **C**) antero-lateral views at embryonic days (ED) 13.5, 14.5 and 15.5. Dark—wild-type (WT) embryos; light—*Spry2*$^{-/-}$ embryos. An epithelial ridge (MS) represents the residuum of the anterior diastemal bud (Fig. 1B), which is most prominent at ED 12.5. $R_2$, posterior diastemal bud; S, supernumerary tooth primordium; $M_1$, enamel organ of the first lower molar. Curved arrow points to the anterior end of the $M_1$ enamel organ, which is closed in controls and open in mutants. Arrowhead indicates the enamel knot area bulging into the mesenchyme. Asterisk shows the position of the connection between S and $M_1$.

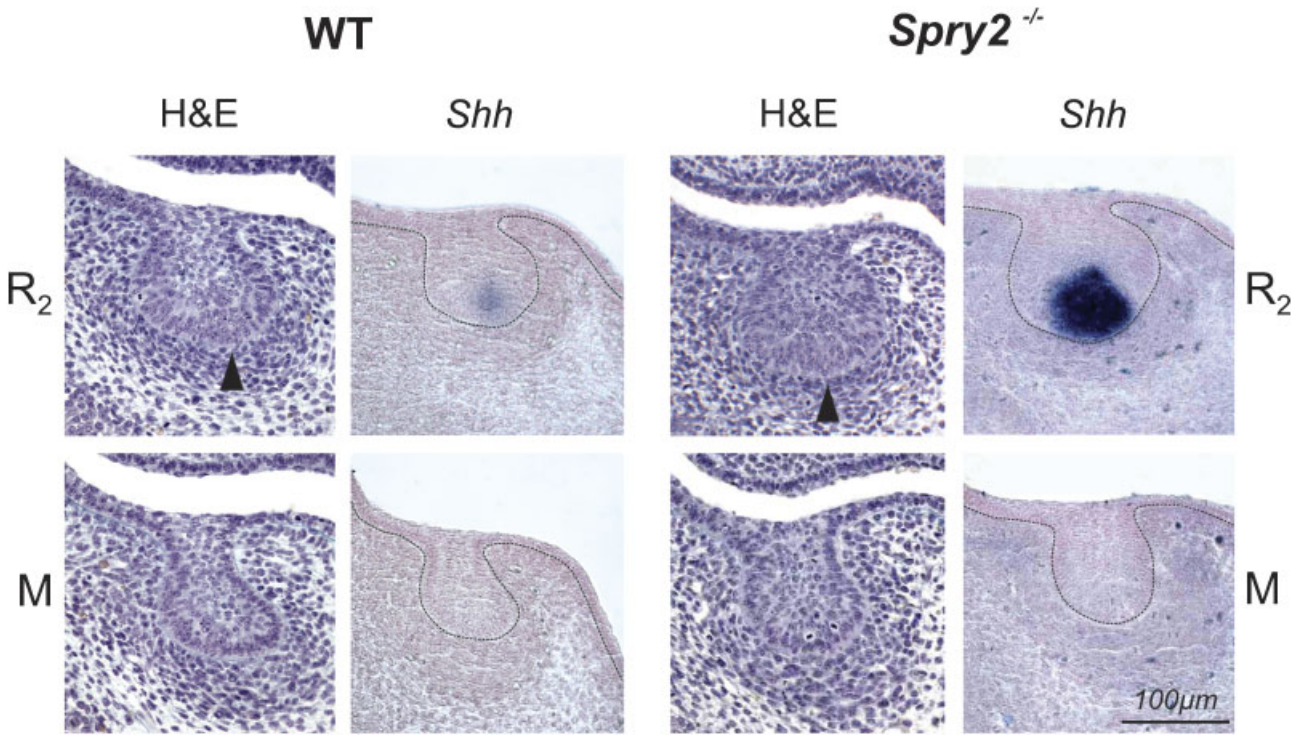


Fig. 4. Dental epithelium on frontal sections of mandible at embryonic day 13.5. In each wild-type (WT) and mutant (*Spry2*$^{-/-}$) embryo, the large posterior diastemal bud ($R_2$) and molar epithelium (M) is presented on histological sections stained with hematoxylin–eosin prestained with alcian blue (H&E) and after *Shh* whole mount in situ hybridization. At the enamel knot area at the tip of the $R_2$ bud (arrowhead) in WT and *Spry2*$^{-/-}$ embryos, *Shh* is expressed, whereas it is absent in the molar epithelium. Note the increased *Shh* expression in the mutant $R_2$ bud.

The apoptotic rate was calculated as the number of apoptotic cells and bodies per square unit ($\times 10^3\,\mu m^2$) of epithelium. This could be determined for individual sections, individual jaw segments or individual groups of jaws (Table 1). Apoptotic cells and bodies were recorded into the drawings of the dental epithelium made from sections (see above-''3D reconstructions''). The size of the dental epithelium on frontal sections was measured using computer software ImageJ (see above-''Morphometry of dental epithelium''). The apoptotic rate was evaluated either in the entire dental epithelium (see the blue+white+red dots in Fig. 6) or separately in the superficial cells (see the blue dots in Fig. 6) and interior cells (see the white and red dots in Fig. 6). Fischer's exact test was used to determine the statistical significance between the total values (Table 1) in a group of WT and mutant tooth primordia.

### *Quantitative evaluation of mitoses*

The proliferation was evaluated at ED 13.5 in the same segments of dental epithelium (Fig. 7) used for the quantitative evaluation of apoptosis (see above). In each section, the total number of epithelial cells and the number of mitotic cells (from early metaphase to early telophase) were counted on digitalized images (at a magnification of $1{,}250\times$) made by Leica DMLB microscope (Leica Microsystems GmbH, Wetzlar, Germany) equipped with a camera Leica DC480 (Leica Microsystems GmbH, Wetzlar, Germany). The mitotic stage was then checked under a $100\times$ immersion objective (Fig. 2). Fischer's exact test was used to determine the statistical significance between the total values (Table 2) in a group of WT and mutant tooth primordia.

### *Whole mount in situ hybridization*

RNA in situ hybridization was performed according to standard protocols on ED 13.5 jaws that were fixed in 4% paraformaldehyde, hybridized in whole mount, embedded in paraffin, sectioned in 10 μm thick frontal sections and counterstained by Nuclear Fast Red (Fluka/Sigma-Aldrich Chemie GmbH, Buchs SG, Switzerland). To generate digoxigenin-labeled probes, we used plasmids containing mouse *Shh* sequences

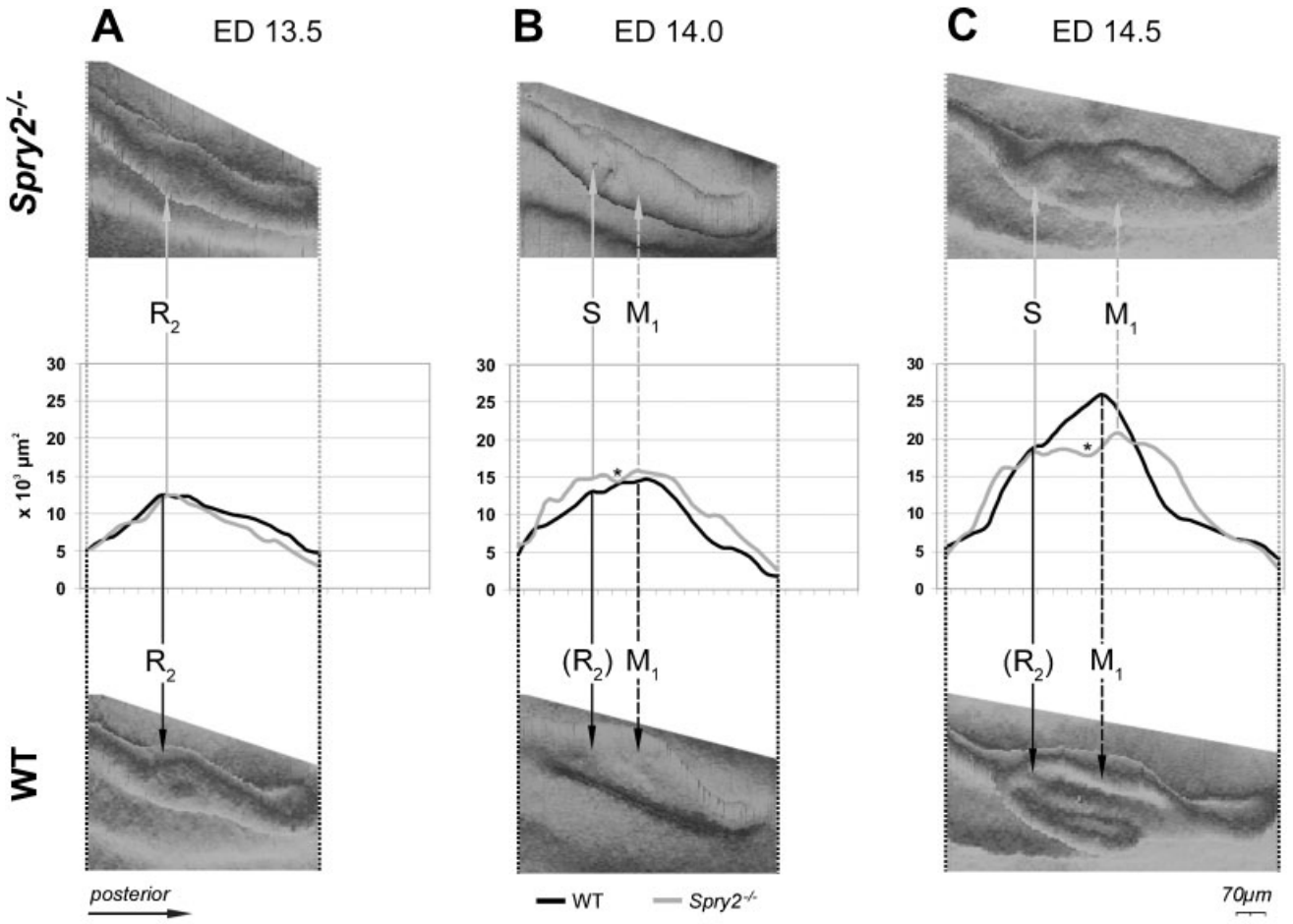


Fig. 5. Changes in size of the dental epithelium along the antero-posterior axis. Graphs depict changes in the area ($\times 10^3\,\mu m^2$) of the dental epithelium measured on frontal sections along the antero-posterior axes in the cheek region of the mandible at embryonic day (ED) 13.5 (**A**), 14.0 (**B**) and 14.5 (**C**). Three-dimensional reconstructions of the measured wild-type and mutant dental epithelium are shown below and above the curves, respectively. Solid arrows point to the position of the posterior diastemal $R_2$ bud at ED 13.5, its estimated position ($R_2$) in WT mice at ED 14.0 and 14.5 or the position of a supernumerary tooth primordium S in mutants at ED 14.0 and 14.5. $M_1$, the first lower molar. Dashed arrow points to the largest region of the $M_1$. Asterisk indicates the area between S and $M_1$. The residuum of the anterior diastemal rudiment (MS-Fig. 1B) is located in front of the $R_2$ bud, and its increased size in *Spry2*$^{-/-}$ embryos is reflected by the anterior part of the anterior elevation on the curve (B, C). WT, wild type.

for in vitro transcription as previously reported (Klein et al., 2006).

## RESULTS

### *Morphogenesis of dental epithelium*

In order to elucidate the relationship between the development of the supernumerary tooth and the morphogenesis of $R_2$ and $M_1$, changes in the size and morphology of the dental epithelium were investigated in the mandibular cheek region from ED 13.5 to 15.5 (Figs. 3–5).

At ED 13.5, the dental epithelium had a bud shape on most frontal sections in WT and *Spry2*$^{-/-}$ embryos (Fig. 4). The bud-shaped dental epithelium on sections corresponded to a ''mound'' shape on 3D reconstructions (Fig. 3A). The morphology and antero-posterior extent of this dental mound were similar in *Spry2*$^{-/-}$ and WT specimens. At the middle part of the epithelial mound, a swelling of the $R_2$ bud (Fig. 1B) was visualized on 3D pictures (Fig. 3A). The anterior part of the swelling included the enamel knot of the $R_2$ (compare with Figs. 4 and 6). The dental epithelium located anteriorly to the $R_2$ bud corresponded to the residuum of the MS rudiment (Fig. 1B), which undergoes regression at ED 13.5. The size (area) of the dental epithelium varied along the antero-posterior axis of the mandible. These changes were similar in WT and *Spry2*$^{-/-}$

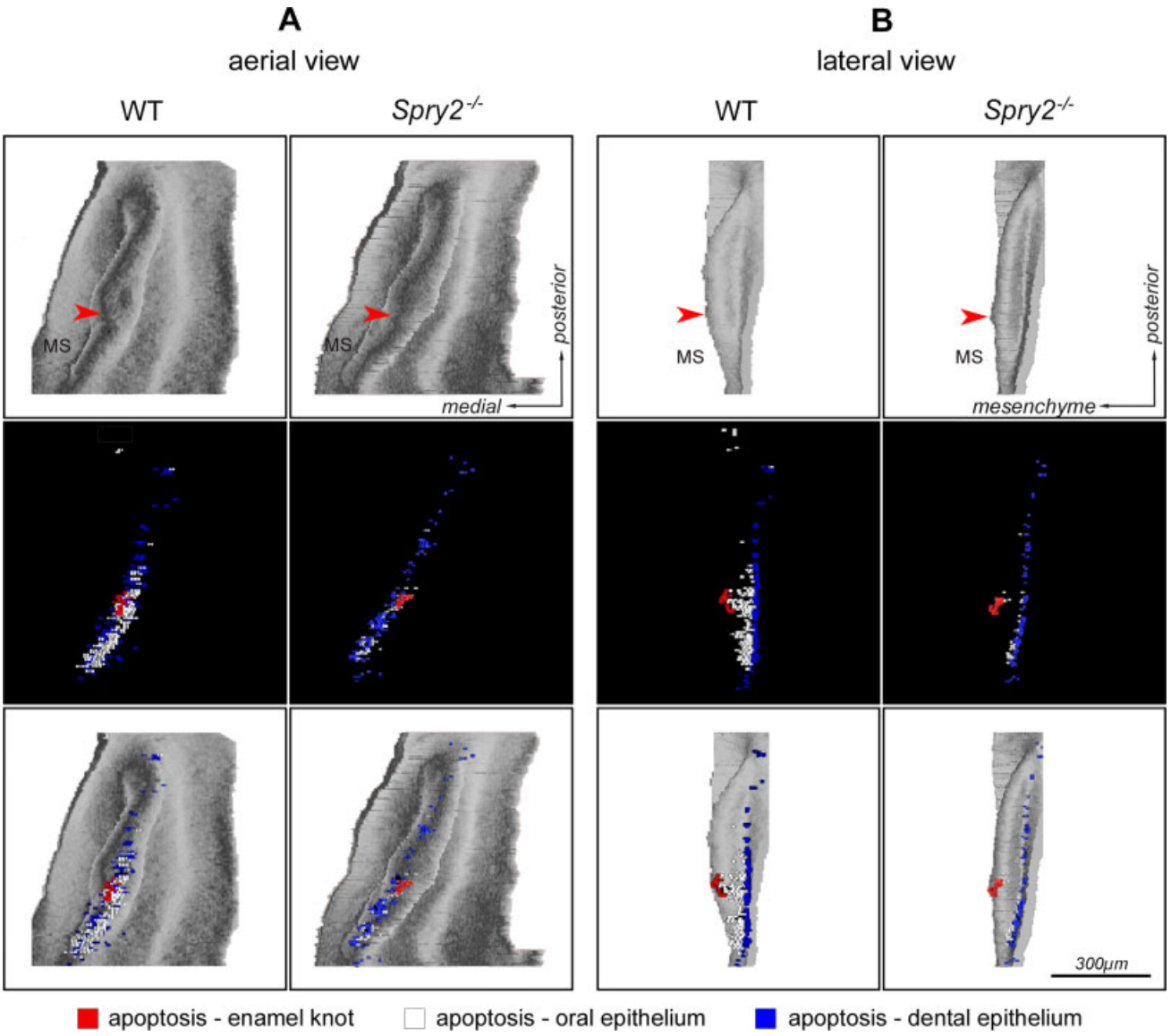


Fig. 6. Distribution of apoptosis in the dental epithelium on 3D reconstructions at embryonic day 13.5. The dental and adjacent oral epithelium in the cheek region of mandible of wild-type (WT) and *Spry2*$^{-/-}$ embryos is presented in (**A**) aerial view or (**B**) lateral view. The first and second rows show the shape of the epithelium and apoptosis distribution, respectively. The third row images are overlays of the first and second rows. Blue and white dots indicate apoptosis in the superficial and internal areas of dental epithelium, respectively. The red dots indicate apoptosis in the enamel knot at the tip (arrowhead) of a wide diastemal bud $R_2$.

embryos (Fig. 5A). The area of the dental epithelium was small anteriorly, gradually increased in the posterior direction until reaching a maximum where the rudimentary bud $R_2$ was located and then decreased. The $R_2$ bud could be identified on frontal sections (Fig. 4) according to its large size, typical shape, increased number of apoptotic bodies and presence of an enamel knot structure at its tip. *Shh* expression was assessed to show that this marker of the enamel knot was indeed expressed at the tip of the $R_2$ bud. The expression was more pronounced in mutants than in controls (Fig. 4).

At ED 14.0–15.5, the antero-posterior length of the dental epithelium increased (Figs. 3 and 5). In contrast to WT mice, where $R_2$ is incorporated into the anterior part of the rapidly growing $M_1$ cap (Viriot et al., 2000), the anterior part of the dental epithelium conspicuously increased in *Spry2*$^{-/-}$ fetuses. It progressively separated from the developing $M_1$ cap, giving rise to the supernumerary tooth primordium (Fig. 3). In comparison with WT

mice, the $M_1$ in age/weight-matched mutants was developmentally retarded (early cap stage) at ED 14.5, and remained open at its anterior end at ED 15.5 (Fig. 3C). The morphometric analysis (Fig. 5) clearly showed that the antero-posterior elongation of the dental epithelium mainly involved a region posterior to the area where the $R_2$ was incorporated into the $M_1$ in controls or where the supernumerary tooth developed in mutants. Although the length of the dental epithelium was similar in stage/weight-matched WT and *Spry2*$^{-/-}$ mice, size differences of the dental epithelium became progressively more evident between control and mutant fetuses (Figs. 3 and 5). In WT mice, only one major elevation was present on the curve. However, its maximum values were higher and located more posteriorly than those at ED 13.5 (Fig. 5). The maximum values reflected the largest middle part of the $M_1$ cap. An accessory peak on the anterior slope on the curve marked the incorporated $R_2$ bud. In contrast, the curves in *Spry2*$^{-/-}$ stage/weight-matched animals showed two elevations separated by a depression (Fig. 5B, C). The anterior elevation reflected the developing supernumerary tooth, whereas the posterior elevation corresponded to the forming $M_1$ cap in mutants (Fig. 3B, C). The maximum values of the anterior elevation were observed at the $R_2$ position (compare Fig. 5A, B). However, this anterior elevation also included the area in front of the $R_2$ (Fig. 5) where the anterior diastemal rudiment MS (Fig. 1B) occurred. Thus, not only the $R_2$ but also the MS was increased in mutants, suggesting that both of these rudiments contribute to the formation of the supernumerary tooth. The depression between the anterior and posterior elevations on the curves in mutants corresponded to the gap between the supernumerary tooth and the $M_1$ primordium (compare Figs. 3B, C and 5B, C). Interestingly, the position of this gap fit into the largest part of $M_1$ in controls (Fig. 5C).

A defect in the segmentation of the dental epithelium along the antero-posterior jaw axes (Peterkova et al., 2002b) was apparent in *Spry2*$^{-/-}$ mandibles. Although the total antero-posterior length of the dental epithelium was similar in

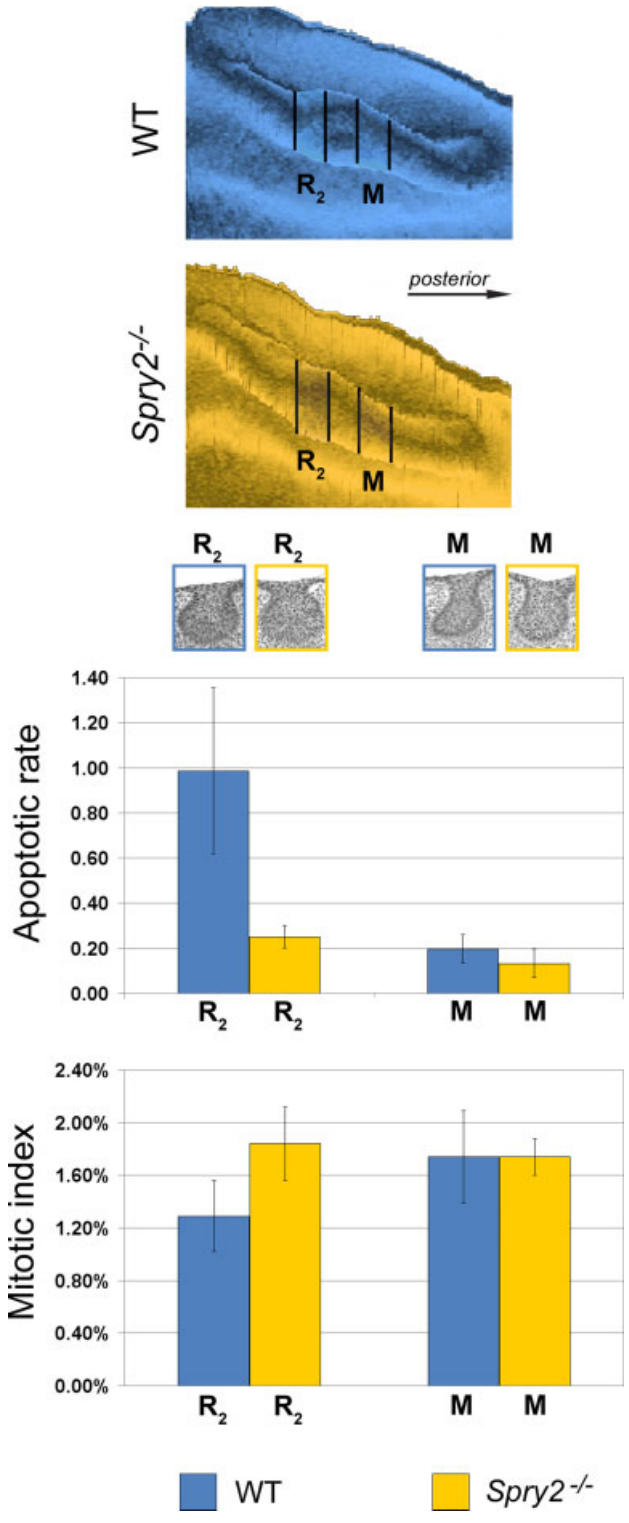


Fig. 7. The apoptotic rate and mitotic index in the $R_2$ bud and molar epithelium at embryonic day 13.5. Two segments of dental epithelium (represented in the aerial view in 3D reconstructions at the top) of wild-type (WT) and *Spry2*$^{-/-}$ embryos were evaluated; colors as in legend. $R_2$ and M refer to the segment of the rudimentary diastemal bud and molar epithelium, respectively. Representative dental epithelia are shown in the frontal sections below the reconstructions, and have been adjusted to the graphs. Compared with the molar region, note the higher level of apoptosis in the $R_2$ in controls, and its dramatic decrease in mutants. In contrast, the mitotic index was significantly lower in the $R_2$ than in the molar region in controls and significantly increased in mutants.

*TABLE 1. Summary of data on the quantitative evaluation of apoptosis*

| | $R_2$ | | | | M | | | |
|---|---|---|---|---|---|---|---|---|
| | Number of sections | Total area ($\mu m^2$) | Total number of apoptotic elements | Apoptotic rate | Number of sections | Total area ($\mu m^2$) | Total number of apoptotic elements | Apoptotic rate |
| *Spry2*$^{-/-}$ | 60 | $800 \times 10^3$ | 201 | $0.25 \times 10^{-3}$ | 60 | $559 \times 10^3$ | 74 | $0.13 \times 10^{-3}$ |
| WT | 100 | $1{,}099 \times 10^3$ | 1,084 | $0.99 \times 10^{-3}$ | 100 | $944 \times 10^3$ | 186 | $0.20 \times 10^{-3}$ |

Apoptotic rate, number of apoptotic elements/$\mu m^2$; $R_2$, the posterior diastema bud in the mandible; M, the molar epithelium in the mandible; WT, wild type.

WT and *Spry2*$^{-/-}$ animals, the anterior boundary of the $M_1$ was located more posteriorly in mutants than in WT mice, because of the presence of a supernumerary tooth anlage (Fig. 5B, C). The distinct separation of the supernumerary tooth primordium from $M_1$ (Fig. 3C) was not observed in all mutant embryos; some specimens only had hyperplasia of the anterior part of the $M_1$ (data not shown).

### *Apoptosis*

In order to test the hypothesis that apoptosis is decreased in the $R_2$ bud in *Spry2*$^{-/-}$ embryos, the distribution of apoptotic bodies and cells (Fig. 2A) was evaluated on frontal sections and represented in 3D reconstructions (Fig. 6) and by quantitative measurements (Table 1, Fig. 7) at ED 13.5.

In WT embryos, apoptosis was mainly concentrated in the anterior part of the dental epithelium, where the diastemal rudiments (MS, $R_2$) were repressed. The apoptotic cells and bodies were abundant in both the internal and superficial cells (see the white and blue dots in Fig. 6), and they were typically located in the enamel knot at the tip of the wide bud $R_2$ (see the red dots in Fig. 6). Interestingly, apoptosis occurred only rarely in the internal cells of the posterior part of the dental epithelium, that is, posterior to the $R_2$ bud (Fig. 6).

In *Spry2* mutants, the apoptotic bodies and cells were also more concentrated in the anterior part of the dental epithelium. However, they were much less abundant in mutant than in WT specimens and were largely absent from the internal parts of the epithelium where both diastemal rudiments were located (see white dots in Fig. 6). In the posterior part of the dental epithelium, the apoptosis distribution did not exhibit a marked difference between WT and mutant specimens and was almost exclusively present in the superficial cells (Fig. 6).

Quantitative evaluation of the number of apoptotic cells and bodies was compared in the $R_2$ bud and the molar epithelium between WT and *Spry2*$^{-/-}$ embryos at ED 13.5 (Table 1, Fig. 7). In the $R_2$ of WT mice, the number of apoptotic cells and bodies was significantly higher ($P < 0.01$) than that in the molar region in both WT and *Spry2*$^{-/-}$ embryos. However, compared with the $R_2$ in WT animals, the number of apoptotic elements (in the whole structure as well as in the internal or superficial parts) was significantly decreased ($P < 0.01$) in the $R_2$ in mutants (Fig. 7). The number of apoptotic elements was also significantly lower ($P < 0.01$) in the molar area of mutants than in WT embryos. The number of apoptotic elements in the mutant $R_2$ did not differ from the molar epithelium in WT embryos ($P > 0.05$).

### *Proliferation*

To assess whether proliferation is increased in the $R_2$ bud of *Spry2* mutant embryos, the mitotic index was evaluated and compared in the $R_2$ bud and the molar epithelium in WT and *Spry2*$^{-/-}$ mandibles at ED 13.5 (Table 2). In WT mandibles, the mitotic index was significantly lower ($P < 0.01$) in the $R_2$ bud than in the molar region. In contrast, the mitotic index in the $R_2$ was significantly higher in *Spry2*$^{-/-}$ than in WT embryos and was similar to that in the molar region. The mitotic index in the molar region showed no significant difference ($P > 0.05$) between WT and mutant jaws (Fig. 7).

## DISCUSSION

We have previously documented that the loss of *Spry2* function leads the diastemal buds to develop into supernumerary teeth (Klein et al., 2006). However, it was not known whether this process occurs as a result of increased proliferation, decreased cell death or both. Here, we show that both decreased apoptosis and increased proliferation were found in the diastemal rudimentary bud $R_2$ (the presumed premolar vestige) in *Spry2*$^{-/-}$ embryos at ED 13.5. This was followed by

*TABLE 2. Summary of data on the quantitative evaluation of proliferation*

| | $R_2$ | | | | M | | | |
|---|---|---|---|---|---|---|---|---|
| | Number of sections | Total number of cells | Total number of mitoses | Mitotic index (%) | Number of sections | Total number of cells | Total number of mitoses | Mitotic index (%) |
| *Spry2*$^{-/-}$ | 60 | 12,151 | 255 | 2.10 | 60 | 8,842 | 175 | 1.98 |
| WT | 100 | 17,131 | 242 | 1.41 | 100 | 13,988 | 279 | 1.99 |

Mitotic index, percentage of mitotic cells in 100 cells; $R_2$, the posterior diastema bud in the mandible; M, the molar epithelium in the mandible; WT, wild type.

hyperplasia of the anterior part of the dental epithelium, where the $R_2$ was located, and by separation of this region from $M_1$, leading to the formation of a supernumerary tooth primordium.

### *Morphogenesis of the dental epithelium*

In WT mice, the initial development of the rudimentary $R_2$ bud, followed by growth retardation and epithelial apoptosis, and finally incorporation into the anterior part of $M_1$, occurred as we previously described (Viriot et al., 2000).

The $R_2$ rudiment has a specific wide-bud shape on frontal sections at ED 13.5 (Fig. 4). In the cheek region, the tooth primordia that have a bud shape on frontal sections appear as ill-defined swellings on a continuous mound of dental epithelium in three dimensions (Fig. 3A) in both mice (Peterkova et al., 2000) and humans (Hovorakova et al., 2005). This dental mound has the appearance of a long cylinder extending along the jaw arch. However, both the epithelial mound and the tooth swellings exhibit a bud shape on frontal sections, and differ primarily in terms of area. This can make it difficult to distinguish tooth primordia from surrounding dental epithelium and explains why the anterior and posterior tooth boundaries are not yet distinct at the bud stage (Hovorakova et al., 2005).

Here, as in previous reports, we observed a swelling on the dental mound in 3D reconstructions at ED 13.5 (Figs. 3A and 5A), which indicated the presence of a distinct bud-stage tooth primordium. Anteriorly, in this swelling, the tip of the $R_2$ bud was marked by the presence of apoptosis (Fig. 6) and had morphological characteristics that are typically present in the enamel knot of the first molar cap (Lesot et al., '96). We suggest that the existence of the $R_2$ primordium as a discrete, active structure can be inferred by the apparent presence of a signaling center, as marked by expression of *Shh* (Fig. 4). *Shh* expression at this location has generally been thought to correspond to the enamel knot of $M_1$ at day 13.

In WT mice, the anterior boundary of the lower $M_1$ becomes apparent at ED 14.5–15.5, when the $M_1$ cap differentiates (Viriot et al., '97) (Fig. 3B, C). However, the well-differentiated enamel organ of the lower $M_1$ at ED 15.5 only corresponds to the anterior two-thirds of the prospective tooth crown (Lesot et al., '99), i.e. to the prospective cusps B1, B2, L1, L2 (terminology by Gaunt, '55). The posterior part of $M_1$ has not yet formed and the enamel organ remains open posteriorly such that the posterior boundary is not yet apparent at ED 15.5 (compare with Fig. 3C). The posterior part of $M_1$ (cusps B3, L3, 4) develops at later stages, long after the primary enamel knot structure of $M_1$ has disappeared (Lesot et al., '99; Obara and Lesot, 2007).

The rudimentary diastemal primordia can advance as far as the bud stage before their arrest (Fig. 1B). Interestingly, the arrest of molar or incisor development in many mouse mutants that lack teeth also occurs at the bud stage (e.g. Peters and Balling, '99). It is not yet known why this is the case, and the identification of factors that regulate physiological tooth arrest in mouse diastemal buds can help to address this question. We have recently shown that the expression of *Spry2* and *Spry4* in the epithelium and mesenchyme, respectively, prevents diastemal tooth formation by making diastemal buds refractory to the FGF signaling that normally sustains tooth development (Klein et al., 2006). The data presented here document the cellular effects of the loss of *Spry2* on morphogenesis. In comparison with the molar region, decreased cell proliferation and increased apoptosis occurred during the physiological growth arrest of the $R_2$ bud in WT embryos. In contrast, both cell proliferation and apoptosis in

the $R_2$ bud remained similar to the molar area in *Spry2* mutants (Fig. 7) and allowed for further growth of the diastemal rudiment.

### *Supernumerary cheek teeth in mice with genetic alterations*

In several mutant or transgenic mice, a supernumerary tooth is found anterior to the first molar. A classical example is the supernumerary cheek tooth in tabby, downless or sleek mutant mice (Gruneberg, '66; Sofaer, '69), which exhibit defects in the EDA signaling pathway (e.g. Elomaa et al., 2001). A supernumerary tooth in front of the first molar has also been reported in $Tg737^{orpk}$ mice (Zhang et al., 2003), in transgenic mice overexpressing the EDA receptor EDAR (Tucker et al., 2004) or the EDA protein itself (Kangas et al., 2004), in ectodin/WISE-deficient mice (Kassai et al., 2005) and in mice homozygous for a null allele of *Spry2* or *Spry4* (Klein et al., 2006).

The supernumerary tooth appears to originate from a rudimentary diastemal bud, whose development is not suppressed as it is in normal mice (Peterkova et al., 2005; Klein et al., 2006). In the case of sprouty null mice, the lack of an FGF antagonist leads to the upregulation of an epithelial–mesenchymal signaling loop that culminates in the formation of a supernumerary tooth in the diastema (Klein et al., 2006).

The incorporation of a rudimentary diastemal bud (Viriot et al., 2000) appears to render the anterior part of the mouse $M_1$ more susceptible to developmental alterations than the rest of the cheek dentition (Boran et al., 2005). The large rudimentary buds in the mouse diastema (Fig. 1B) have been hypothesized to represent vestiges of ancestral premolars suppressed during evolution (Peterkova et al., 2000; Viriot et al., 2002). We have proposed that the incorporation of the rudimentary diastemal bud (premolar vestige) into the $M_1$ fails in some mouse mutants and that the rudiment takes part in the formation of a supernumerary tooth. Such a tooth in front of the first molar in mutant mice might be, at least in part, homologous to a premolar lost during the evolution of muroids, and can be thought of as an evolutionary throwback (atavism) (Peterkova et al., 2005, 2006). This hypothesis is supported by (1) the development and incorporation of the $R_2$ bud into the lower $M_1$ in WT mice (Viriot et al., 2000), (2) the concentration of apoptotic cells and bodies in the anterior part of the dental epithelium in WT mice at early and later prenatal stages (Viriot et al., 2000; Boran et al., 2005), (3) the origin of a supernumerary tooth primordium in the location of $R_2$ in tabby homo/hemizygous embryos (Peterkova et al., 2002b, 2005) and (4) paleontological data, as follows. During the evolution of muroid rodents (about 50 million years ago), the disappearance of the last premolar correlated with the extension of the anterior part of the first lower molar (Viriot et al., 2002). Thus, mutant mice with a supernumerary tooth in front of $M_1$ are more similar in terms of dentition to nonmuroid rodents with maintained premolars than are WT mice (Peterkova et al., 2005, 2006).

If a rudimentary bud participates in the development of the anterior part of $M_1$ in WT mice, then the anterior domain of $M_1$ should be reduced when the rudimentary bud is involved in the formation of a supernumerary tooth in mutants. Indeed, a number of studies document such a reduction in the anterior part of $M_1$ adjacent to a supernumerary tooth in mice with different genetic alterations (e.g. Gruneberg, '66; Kangas et al., 2004; Tucker et al., 2004; Kassai et al., 2005). This reduction has been proposed to result from the inhibitory influence of the developing supernumerary tooth (e.g. Sofaer, '75). However, our previous study (Peterkova et al., 2002b, 2005) has clearly shown that the supernumerary tooth in tabby homo/hemizygous mice forms where the diastemal bud is incorporated into the anterior part of the $M_1$ cap in WT mice. This is followed by a defect in the segmentation of the dental epithelium: the total antero-posterior length of the dental epithelium is similar in WT and mutant embryos. However, this epithelium is differently distributed to give rise to tooth primordia. The larger the most anterior (supernumerary) tooth primordium, the shorter, more posteriorly located and developmentally less advanced are the successive cheek teeth. Consequently, the positions of tooth boundaries do not match those of the WT molars (Peterkova et al., 2002b, 2005). This reciprocal correlation between the length of the first cheek tooth and the second or third tooth, together with a stable total length of the dental row, has also been reported in adult tabby homo/hemizygous mice (Kristenova et al., 2002). The existence of size interactions between molar teeth in mice has been proposed and led to the conclusion that the first molar controls the ultimate form of the whole molar row, which tends to maintain a stable length (Gruneberg, '65; Sofaer, '69; Kavanagh et al., 2007).

A defect in the segmentation of the dental epithelium was also found in the *Spry2*$^{-/-}$ embryos reported here. In a similar antero-posterior length of the dental epithelium, $M_1$ only developed in controls, whereas both supernumerary tooth and $M_1$ primordia developed in mutants at early stages (Figs. 3 and 5). The supernumerary tooth originated in the location that corresponded to the anterior part of the control $M_1$. The mutant $M_1$ was located more posteriorly and exhibited a reduction in its anterior part, where the enclosure by the cervical loop was missing (Fig. 3C). Despite these marked prenatal differences, the adult lower $M_1$ adjacent to the supernumerary tooth is surprisingly almost completely normal in *Spry2*$^{-/-}$ mice (Klein et al., 2006). In these cases, the supernumerary tooth does not develop at the expense of $M_1$, but has to include some additional material at the anterior end of $M_1$, which is not normally present there. A large supernumerary tooth in front of an almost normal $M_1$ occurs in some tabby heterozygous mice, and the anterior diastemal rudiment MS (Fig. 1B) is thought to take a part in its origin (Peterkova et al., 2005). It is possible that the MS rudiment, in addition to the $R_2$, participates in the morphogenesis of the supernumerary tooth in *Spry2*$^{-/-}$ embryos. This is indicated by the increased size of the epithelium (Fig. 5A) and decreased amount of apoptosis (Fig. 6) in both $R_2$ and MS in these mutants. The specific roles of each of these diastemal rudiments in the origin of supernumerary teeth in sprouty mutants will be the focus of future studies.

### *Apoptosis*

In WT embryonic mouse mandibles apoptosis concentrates in the anterior part of the dental epithelium in the cheek region, where the large diastemal buds have arrested (Viriot et al., 2000). At ED 13.5, apoptosis is also specifically located in the enamel knot (see below), which is transiently present at the tip of the $R_2$ (Peterkova et al., 2002a). The concentration of apoptosis in the anterior part of the $M_1$ epithelium is present during cap formation, which points to the incorporation of the $R_2$ bud there (Viriot et al., 2000).

As the development continues, apoptosis remains concentrated at the base of the anterior part of the $M_1$ at late cap and early bell stages (Viriot et al., '97; Boran et al., 2005). This suggests that, although incorporated into the $M_1$, the $R_2$ epithelium (the presumptive premolar vestige) is somehow distinct from the rest of the molar in WT mice and represents a ''locus minoris resistentiae,'' a region that is prone to developmental anomalies in genetically altered mice (Boran et al., 2005).

During further tooth development, apoptosis is specifically concentrated in the primary enamel knot of $M_1$, which is a cluster of epithelial cells located in the middle of the molar cap and adjacent to the papilla mesenchyme (Fig. 3B) (Butler, '56; Lesot et al., '96). The enamel knot is thought to play an important role during tooth morphogenesis (Bolk, '22; Butler, '56; MacKenzie et al., '92; Jernvall et al., '94, '98; Lesot et al., '96, '99; Vaahtokari et al., '96a; Coin et al., '99, 2000a). Interestingly, although caspase-3, caspase-9 and APAF-1 are all thought to be involved in the regulation of apoptosis in the molar enamel knot, these do not seem to be required for molar tooth formation (Matalova et al., 2006; Setkova et al., 2007). Similarly, inhibition of apoptosis in the primary enamel knot using a caspase inhibitor (Z-VAD-fmk) in vitro does not affect mouse tooth crown morphogenesis (Coin et al., 2000b). These studies focused exclusively on apoptosis in the enamel knot in the middle part of the $M_1$ cap. No experimental data are available regarding the regulation or effect of inhibition of apoptosis during development of the large diastemal buds (Peterkova et al., 2003).

We demonstrated that the absence of *Spry2*, by changing the equilibrium between growth activators and inhibitors (Fig. 1C), leads to a revival of a diastemal bud owing to the downregulation of apoptosis and increased proliferation (Fig. 7). As a consequence, the anterior part of the dental epithelium in the cheek region of the mandible was more abundant. Instead of growth arrest of the diastemal buds and incorporation of $R_2$ into $M_1$, as is found in WT mice, the rudimentary dental epithelium was revitalized and tended to separate from $M_1$, forming an independent, supernumerary tooth (Figs. 3 and 5).

### *Molecular considerations*

We have proposed a hypothesis to explain the regulation of epithelial apoptosis during tooth formation by integrating two concepts (Peterkova et al., 2003): (1) The reaction/diffusion model of budding morphogenesis controlled by the relative balance of growth-activating and -inhibiting signals (for a review, see Peterkova et al., 2000, 2002a), and (2) a model of apoptosis regulation by

the relative balance between death-suppressing and death-stimulating signals (Raff, '92) (Fig. 1C).

It appears that FGF signaling from dental mesenchyme to epithelium is increased in *Spry2*$^{-/-}$ mice because of the absence of Spry2 in the epithelium. This is probably owing to increased sensitivity to FGF10, which is only weakly expressed in diastemal mesenchyme in WT mice, and to FGF3 from the adjacent first molar. In contrast, *Fgf10* and *Fgf3* are strongly expressed in the $M_1$ mesenchyme in WT mice (e.g. Klein et al., 2006). As a consequence of inactivation of *Spry2*, there is more intense *Shh* expression in the signaling center of the diastemal bud in mutant than in WT embryos (Fig. 4). It is also striking that *Fgf4* expression is seen in the diastemal bud in mutants, as this has never been seen in controls (Klein et al., 2006). Thus, it is possible that FGF4 is a direct or indirect target of SHH signaling.

The epithelial *Fgf4* expression is under the control of the transcription factor LEF1, which is an effector of canonical Wnt signaling. It has previously been shown that FGF4 added exogenously to cultured isolated WT dental mesenchyme prevents apoptosis (Vaahtokari et al., '96b) in the dental epithelium of *Lef1*$^{-/-}$ mice (Sasaki et al., 2005). In *Lef1*$^{-/-}$ embryos, tooth development is arrested at the bud stage (Kratochwil et al., 2002). EDA, which promotes tooth development, is also under the control of LEF1 (Laurikkala et al., 2001), and EDA can upregulate *Shh* expression in ectodermal derivatives (Pummila et al., 2007). These data suggest that the level of EDA signaling could be a key parameter that controls *Shh* expression. We hypothesize that the upregulation of FGF signaling stabilizes tooth bud development by stimulating the canonical Wnt signaling pathway, which reinforces *Fgf4*, *Shh* and *Eda* expression. These latter molecules then act as growth activators in the epithelium.

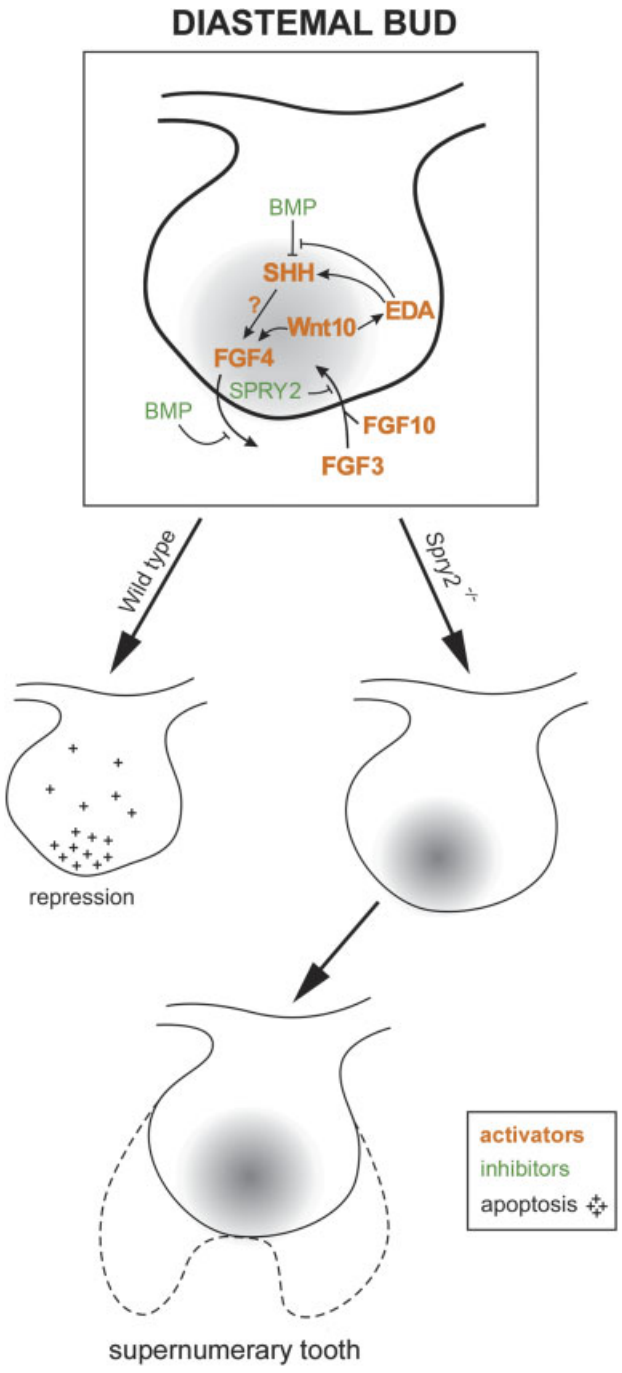


Fig. 8. Model of revitalization of a diastemal bud. A drawing of a posterior diastemal bud ($R_2$) at ED 13.5 with a signaling center (gray) at its tip (compare with Fig. 3). Growth inhibitors (e.g. BMP) and growth activators (e.g. SHH, Wnt10, FGF3, FGF4, FGF10, EDA) are distinguished by colors, as in legend (compare with Fig. 1C). We propose that FGF signaling from the mesenchyme can induce expression of FGF4, SHH and EDA, perhaps by the stimulation of the Wnt/LEF1 pathway, and SPRY2 can antagonize this cascade. In wild-type diastemal buds, *Spry2* is expressed, the growth-activation pathway is blocked and bud growth is stopped by a relative prevalence of growth inhibitors. The mitotic index is decreased and apoptosis occurs in the epithelium (crosses). In *Spry2* mutants, development of the rudimentary bud is not arrested. In contrast to WT embryos, apoptosis is decreased in the rudimentary bud, whereas its mitotic index is as high as in the molar region. Determination of the extent of the contribution of the $R_2$ rudiment to the supernumerary tooth will require future studies. This model is based on findings reported in this study and on previously reported studies (Hogan, '99; Peterkova et al., 2000, 2003; Zhang et al., 2000; Laurikkala et al., 2001; Kratochwil et al., 2002; Nadiri et al., 2004; Klein et al., 2006; Pummila et al., 2007). ED, embryonic day; BMP, bone morphogenetic protein; FGF, fibroblast growth factor; SHH, Sonic hedgehog; EDA, ectodysplasin; SPRY, sprouty; LEF, lymphoid enhancer binding factor.

Bone morphogenetic proteins (BMPs) can act as growth inhibitors during epithelial budding in feathers, hair and lungs (Hogan, '99), during tooth cusp formation (Weiss et al., '98; Jernvall and Thesleff, 2000) and during budding of rudimentary tooth primordia (Peterkova et al., 2000). BMPs have been detected in the epithelium and mesenchyme at the bud stage of tooth development (Tureckova et al., '95; Vaahtokari et al., '96a; Nadiri et al., 2004) and stimulate apoptosis and inhibit growth in the dental epithelium (Tureckova et al., '96; Vaahtokari et al., '96b; Jernvall et al., '98; Peterkova et al., 2003). In addition, BMP4 is able to inhibit *Shh* expression in tooth primordia culture (Zhang et al., 2000). The BMPs appear to inhibit growth in two ways: by affecting the SHH and/or FGF signaling pathways and by promoting cell cycle arrest (Fig. 8). BMP4 activity can be blocked by the EDA pathway, as this pathway can increase the expression of BMP inhibitors such as CCN2 and follistatin (Pummila et al., 2007). Thus, EDA can exert its growth-activation effect either by the stimulation of *Shh* expression or by the inhibition of BMPs (Fig. 8).

## CONCLUDING STATEMENT

In summary, our data have documented for the first time that *Shh* is expressed in the rudimental diastemal $R_2$ bud at ED 13.5. We demonstrated using quantitative techniques that the $R_2$ structure, which is often thought to be $M_1$ at ED 13.5, is arrested in WT mice owing to significantly increased apoptosis and decreased proliferation compared with the molar region. In contrast, the growth arrest of the $R_2$ was prevented in *Spry2* null mice by the upregulated FGF signaling. There the epithelial proliferation and apoptosis in the $R_2$ rudiment remained similar to the molar area. Instead of undergoing arrest and incorporation into the $M_1$ cap at ED 14–15, as it is in WT mice, the $R_2$ was revitalized and involved in the formation of the supernumerary tooth in mutants. These changes show that the evolutionary suppression of the premolar anlage can be rescued by a relative predominance of growth activators (such as FGF, EDA or SHH) over growth inhibitors.

Our studies may represent an alternative to tooth tissue engineering (Duailibi et al., 2006; Hu et al., 2006; Yen and Sharpe, 2006) by raising the stimulating possibility that the rudimental tooth structures can serve as models of controlled tooth regeneration (Peterkova et al., 2006; D'Souza and Klein, 2007). It is indeed possible that the reactivation of the dental lamina to form teeth, as shown here with an embryonic diastemal element, can be extended to other regions of the jaw and to other timepoints in development or adult life.

## ACKNOWLEDGMENTS

We thank Iva Koppova, Zdenka Lisa, J. Fluck and David Lyons for their excellent technical assistance, and Dr. Gail Martin for the support and encouragement during these studies. O. K. was supported by a grant from the NIH (K08-DE017654).

## LITERATURE CITED

Bolk L. 1922. Odontological essays. On the relation between reptilian and mammalian teeth. J Anat 56:107–136.

Boran T, Lesot H, Peterka M, Peterkova R. 2005. Increased apoptosis during morphogenesis of the lower cheek teeth in tabby/EDA mice. J Dent Res 84:228–233.

Butler PM. 1956. The ontogeny of molar teeth. Biol Rev 31:30–70.

Celli G, Larochelle WJ, Mackem S, Sharp R, Merlino G. 1998. Soluble dominant-negative receptor uncovers essential roles for fibroblast growth factors in multi-organ induction and patterning. EMBO J 17:1642–1655.

Coin R, Lesot H, Vonesch JL, Haikel Y, Ruch JV. 1999. Aspects of cell proliferation kinetics of the dental epithelium during mouse molar and incisor morphogenesis: a reappraisal of the role of the enamel knot area. Int J Dev Biol 43:261–267.

Coin R, Schmitt R, Lesot H, Vonesch JL, Ruch JV. 2000a. Regeneration of halved embryonic lower first mouse molars: correlation with the distribution pattern of non dividing IDE cells, the putative organizers of morphogenetic units, the cusps. Int J Dev Biol 44:289–295.

Coin R, Kieffer S, Lesot H, Vonesch JL, Ruch JV. 2000b. Inhibition of apoptosis in the primary enamel knot does not affect specific tooth crown morphogenesis in the mouse. Int J Dev Biol 44:389–396.

D'Souza RN, Klein OD. 2007. Unraveling the molecular mechanisms that lead to supernumerary teeth in mice and men: current concepts and novel approaches. Cells Tissues Organs 186:60–69.

Duailibi SE, Duailibi MT, Vacanti JP, Yelick PC. 2006. Prospects for tooth regeneration. Periodontol 2000 41: 177–187.

Elomaa O, Pulkkinen K, Hannelius U, Mikkola M, Saarialho-Kere U, Kere J. 2001. Ectodysplasin is released by proteolytic shedding and binds to the EDAR protein. Hum Mol Genet 10:953–962.

Gaunt WA. 1955. The development of the molar pattern of the mouse (*Mus musculus*). Acta Anat (Basel) 24:249–268.

Gruneberg H. 1965. Genes and genotypes affecting the teeth of the mouse. J Embryol Exp Morphol 14:137–159.

Gruneberg H. 1966. The molars of the tabby mouse, and a test for the 'single-active X-chromosome' hypothesis. J Embryol Exp Morphol 15:223–244.

Hogan BLM. 1999. Morphogenesis. Cell 96:225–233.

Hovorakova M, Lesot H, Peterka M, Peterkova R. 2005. The developmental relationship between the deciduous dentition and the oral vestibule in human embryos. Anat Embryol 209:303–313.

Hu B, Nadiri A, Kuchler-Bopp S, Perrin-Schmitt F, Peters H, Lesot H. 2006. Tissue engineering of tooth crown, root, and periodontium. Tissue Eng 12:2069–2075.

Jernvall J, Thesleff I. 2000. Reiterative signaling and patterning during mammalian tooth morphogenesis. Mech Dev 92:19–29.

Jernvall J, Kettunen P, Karavanova I, Martin LB, Thesleff I. 1994. Evidence for the role of the enamel knot as a control center in mammalian tooth cusp formation: non-dividing cells express growth stimulating Fgf-4 gene. Int J Dev Biol 38:463–469.

Jernvall J, Åberg T, Ketunen P, Keranen S, Thesleff I. 1998. The life history of an embryonic signaling center: BMP-4 induces p21 and is associated with apoptosis in the mouse tooth enamel knot. Development 125:161–169.

Kangas AT, Evans AR, Thesleff I, Jernvall J. 2004. Non-independence of mammalian dental characters. Dev Biol 268:185–194.

Kassai Y, Munne P, Hotta Y, Penttila E, Kavanaghagh K, Ohbayashi N, Takada S, Thesleff I, Jernvall J, Itoh N. 2005. Regulation of mammalian tooth cusp patterning by ectodin. Science 309:2067–2070.

Kavanagh KD, Evans AR, Jernvall J. 2007. Predicting evolutionary patterns of mammalian teeth from development. 449:427–432.

Klein OD, Minowada G, Peterkova R, Kangas A, Yu BD, Lesot H, Peterka M, Jernvall J, Martin GR. 2006. Sprouty genes control diastema tooth development via bidirectional antagonism of epithelial–mesenchymal FGF signaling. Dev Cell 11:181–190.

Klein OD, Lyons DB, Balloch G, Marshall GW, Basson MA, Peterka M, Boran T, Peterkova R, Martin GR. 2008. An FGF signaling loop sustains the generation of differentiated progeny from stem cells in mouse incisors. Development 135:377–385.

Kratochwil K, Galceran J, Thontsch S, Roth W, Grosschedl R. 2002. FGF4, a direct target of LEF1 and Wnt signaling, can rescue the arrest of tooth organogenesis in Lef1(−/−) mice. Genes Dev 16:3173–3185.

Kristenova P, Peterka M, Lisi S, Gendrault JL, Lesot H, Peterkova R. 2002. Different morphotypes of functional dentition in the lower molar region of tabby (EDA) mice. Orthod Craniofac Res 5:205–214.

Laurikkala J, Mikkola M, Mustonen T, Aberg T, Koppinen P, Pispa J, Nieminen P, Galceran J, Grosschedl R, Thesleff I. 2001. TNF signaling via the ligand–receptor pair ectodysplasin and edar controls the function of epithelial signaling centers and is regulated by Wnt and activin during tooth organogenesis. Dev Biol 229:443–455.

Lesot H, Vonesch JL, Peterka M, Tureckova J, Peterkova R, Ruch JV. 1996. Mouse molar morphogenesis revisited by three dimensional reconstruction: II) spatial distribution of mitoses and apoptosis in cap to bell stages first and second molar teeth. Int J Dev Biol 40:1017–1031.

Lesot H, Peterkova R, Schmitt R, Meyer JM, Viriot L, Vonesch JL, Senger B, Peterka M, Ruch JV. 1999. Initial features of the inner dental epithelium histomorphogenesis in the first lower molar in mouse. Int J Dev Biol 43:245–254.

MacKenzie A, Ferguson MW, Sharpe PT. 1992. Expression patterns of the homeobox gene, Hox-8, in the mouse embryo suggest a role in specifying tooth initiation and shape. Development 115:403–420.

Matalova E, Sharpe PT, Lakhani SA, Roth KA, Flavell RA, Setkova J, Misek I, Tucker AS. 2006. Molar tooth development in caspase-3 deficient mice. Int J Dev Biol 50: 491–497.

Minowada G, Jarvis LA, Chi CL, Neubuser A, Sun X, Hacohen N, Krasnow MA, Martin GR. 1999. Vertebrate Sprouty genes are induced by FGF signaling and can cause chondrodysplasia when overexpressed. Development 126: 4465–4475.

Nadiri A, Kuchler-Bopp S, Haikel Y, Lesot H. 2004. Immunolocalization of BMP-2/-4, FGF-4, and WNT10b in the developing mouse first lower molar. J Histochem Cytochem 52:103–112.

Nie X, Luukko K, Kettunen P. 2006. FGF signalling in craniofacial development and developmental disorders. Oral Dis 12:102–111.

Obara N, Lesot H. 2007. Asymmetrical growth, differential cell proliferation, and dynamic cell rearrangement underlie epithelial morphogenesis in mouse molar development. Cell Tissue Res 330:461–473.

Peterka M, Lesot H, Peterkova R. 2002. Body weight in mouse embryos specifies staging of tooth development. Connect Tissue Res 43:186–190.

Peterkova R, Peterka M, Vonesch JL, Ruch JV. 1995. Contribution of 3-D computer assisted reconstructions to the study of the initial steps of mouse odontogenesis. Int J Dev Biol 39:239–247.

Peterkova R, Lesot H, Vonesch JL, Peterka M, Ruch JV. 1996. Mouse molar morphogenesis revisited by three dimensional reconstruction: I) analysis of initial stages of the first upper molar development revealed two transient buds. Int J Dev Biol 40:1009–1016.

Peterkova R, Peterka M, Viriot L, Lesot H. 2000. Dentition development and budding morphogenesis. J Craniofac Genet Dev Biol 20:158–172.

Peterkova R, Peterka M, Viriot L, Lesot H. 2002a. Development of the vestigial tooth primordia as part of mouse odontogenesis. Connect Tissue Res 43:120–128.

Peterkova R, Kristenova P, Lesot H, Lisi S, Vonesch JL, Gendrault JL, Peterka M. 2002b. Different morphotypes of the tabby (EDA) dentition in the mouse mandible result from a defect in the mesio-distal segmentation of dental epithelium. Orthod Craniofac Res 5:215–226.

Peterkova R, Peterka M, Lesot H. 2003. The developing mouse dentition: a new tool for apoptosis study. Ann N Y Acad Sci 1010:453–466.

Peterkova R, Lesot H, Viriot L, Peterka M. 2005. The supernumerary cheek tooth in tabby/EDA mice—a reminiscence of the premolar in mouse ancestors. Arch Oral Biol 50:219–225.

Peterkova R, Lesot H, Peterka M. 2006. Phylogenetic memory of developing mammalian dentition. J Exp Zoolog B Mol Dev Evol 306:234–250.

Peters H, Balling R. 1999. Teeth. Where and how to make them. Trends Genet 15:59–65.

Pummila AM, Fliniaux I, Jaatinen R, James MJ, Laurikkala J, Schneider P, Thesleff I, Mikkola ML. 2007. Ectodysplasin has a dual role in ectodermal organogenesis: inhibition of Bmp activity and induction of Shh expression. Development 134:117–125.

Raff MC. 1992. Social controls on cell survival and cell death. Nature 356:397–400.

Sasaki T, Ito Y, Xu X, Han J, Bringas Jr P, Maeda T, Slavkin HC, Groschedl R, Chai Y. 2005. LEF1 is a critical epithelial survival factor during tooth morphogenesis. Dev Biol 278:130–143.

Setkova J, Matalova E, Sharpe PT, Misek I, Tucker AS. 2007. Primary enamel knot cell death in Apaf-1 and caspase-9 deficient mice. Arch Oral Biol 52:15–19.

Shim K, Minowada G, Coling DE, Martin GR. 2005. Sprouty2, a mouse deafness gene, regulates cell fate decisions in the auditory sensory epithelium by antagonizing FGF signaling. Dev Cell 8:553–564.

Sofaer JA. 1969. Aspects of the tabby-crinkled-downless syndrome. I. The development of tabby teeth. J Embryol Exp Morphol 22:181–205.

Sofaer JA. 1975. Interaction between tooth germs and the adjacent dental lamina in the mouse. Arch Oral Biol 20:57–61.

Tucker AS, Headon DJ, Courtney JM, Overbeek P, Sharpe PT. 2004. The activation level of the TNF family receptor, Edar, determines cusp number and tooth number during tooth development. Dev Biol 268:185–194.

Tureckova J, Sahlberg C, Aberg T, Ruch JV, Thesleff I, Peterkova R. 1995. Comparison of expression of the msx-1, msx-2, BMP-2 and BMP-4 genes in the mouse upper diastemal and molar tooth primordia. Int J Dev Biol 39:459–468.

Tureckova J, Lesot H, Vonesch JL, Peterka M, Peterkova R, Ruch JV. 1996. Apoptosis is involved in the disappearance of the diastemal dental primordia in mouse embryo. Int J Dev Biol 40:483–489.

Vaahtokari A, Åberg T, Jernvall J, Keränen S, Thesleff I. 1996a. The enamel knot as a signaling center in the developing mouse tooth. Mech Dev 54:39–43.

Vaahtokari A, Åberg T, Thesleff I. 1996b. Apoptosis in the developing tooth: association with an embryonic signaling center and suppression by EGF and FGF-4. Development 122:121–129.

Viriot L, Peterkova R, Vonesch JL, Peterka M, Ruch JV, Lesot H. 1997. Mouse molar morphogenesis revisited by three dimensional reconstruction: III) spatial distribution of mitoses and apoptoses up to bell-staged first lower molar teeth. Int J Dev Biol 41:679–690.

Viriot L, Lesot H, Vonesch JL, Ruch JV, Peterka M, Peterkova R. 2000. The presence of rudimentary odontogenic structures in the mouse embryonic mandible requires reinterpretation of developmental control of first lower molar histomorphogenesis. Int J Dev Biol 44:233–240.

Viriot L, Peterkova R, Peterka M, Lesot H. 2002. Evolutionary implications of the occurrence of two vestigial tooth germs during early odontogenesis in the mouse lower jaw. Connect Tissue Res 43:129–133.

Weiss KM, Stock DW, Zhao Z. 1998. Dynamic interactions and the evolutionary genetics of dental patterning. Crit Rev Oral Biol Med 9:369–398.

Yen AH, Sharpe PT. 2006. Regeneration of teeth using stem cell-based tissue engineering. Expert Opin Biol Ther 6:9–16.

Zhang Y, Zhang Z, Zhao X, Yu X, Hu Y, Geronimo B, Fromm SH, Chen YP. 2000. A new function of BMP4: dual role for BMP4 in regulation of Sonic hedgehog expression in the mouse tooth germ. Development 127:1431–1443.

Zhang Q, Murcia NS, Chittenden LR, Richards WG, Michaud EJ, Woychik RP, Yoder BK. 2003. Loss of the Tg737 protein results in skeletal patterning defects. Dev Dyn 27:78–90.